16th World Conference on Earthquake, 16WCEE 2017

Santiago Chile, January 9th to 13th 2017

Paper N° 2610

Registration Code: S-P1463230164

EVALUATION OF SEISMIC RESPONSES OF BUILDING SYSTEMS WITH SELF-CENTERING CONCRETE STRUCTURAL WALLS

R. Salinas [1], M. Rodríguez [2], R. Sánchez [3]

[1] *Associated Professor, Japan-Peru Center for Earthquake Engineering Research and Disaster Mitigation, Faculty of Civil Engineering, National University of Engineering, Lima, Perú, rsalinas@uni.edu.pe*
[2] *Professor, Institute of Engineering, National University of Mexico, México D.F., México, mrod@unam.mx*
[3] *Auxiliary Professor, Faculty of Civil Engineering, National University of Engineering, Lima, Perú, rsanchezm@uni.edu.pe*

Abstract

Currently, the development of seismic design and construction procedures is oriented toward reducing damages in structures and in building equipment in response to various levels of earthquake intensity. Among the innovative strategies proposed to reduce damages in structures, the use of structural elements with precast concrete and self-centering walls has been proposed. A self-centering wall is defined as a reinforced concrete wall on a foundation with post-tensioned tendons fixed to the foundation and without a monolithic joint between the wall and the foundation. Some ductile steel bars are included at the base of the wall for energy dissipation and for the formation of a hybrid system. Behavior of precast walls with unbonded post-tensioned tendons has been studied by several authors by tests that showed some capabilities of systems with unbonded post-tensioned tendons, such as self-centering response and decreased residual displacements.

This paper describes the results of shaking table tests of three five-story miniature buildings with dual (wall–frame) systems, designed with seismic design criteria similar to those used in conventional dual systems. Two tests units had self-centering reinforced concrete structural walls, and one test unit had a conventional reinforced concrete structural wall. The self-centering walls were built with unbonded post-tensioning tendons and energy dissipators of ASTM A615 steel joining the wall base and the wall foundation. The tests showed that the test units with self-centering dual systems behaved in a manner similar to the test unit with the conventional dual system. In addition, an increase in the participation of the self-centering structural walls in the total seismic response was observed to lead to an increase in overstrength and a decrease in residual drifts of the structure, as well as a decrease in residual deformations in critical sections of the frame elements.

Keywords: Shaking table test; Self-centering walls; Wall-frame systems; Reinforced concrete structures.

1. Introduction

A self-centering wall is defined as an RC wall on a foundation with unbonded post-tensioning tendons fixed to the foundation and without a monolithic joint between the wall and the foundation. Ductile steel bars are included at the base of the wall for energy dissipation and for the formation of a hybrid system (Fig. 1). Most studies of self-centering walls reported in the literature were oriented toward defining the inelastic and elastic characteristics of the force–displacement relationships of self-centering walls as isolated structural elements [1, 2, 3, 4]. In the last decade, the behavior of precast walls with unbonded post-tensioned tendons has been studied by several authors [5, 6, 7, 8].

This paper describes results of shaking table tests of three five-story miniature buildings with dual systems (wall–frame combinations). One of the buildings had a conventional RC structural wall and the other two had self-centering RC structural walls with unbonded post-tensioning tendons and energy dissipators at the wall base.

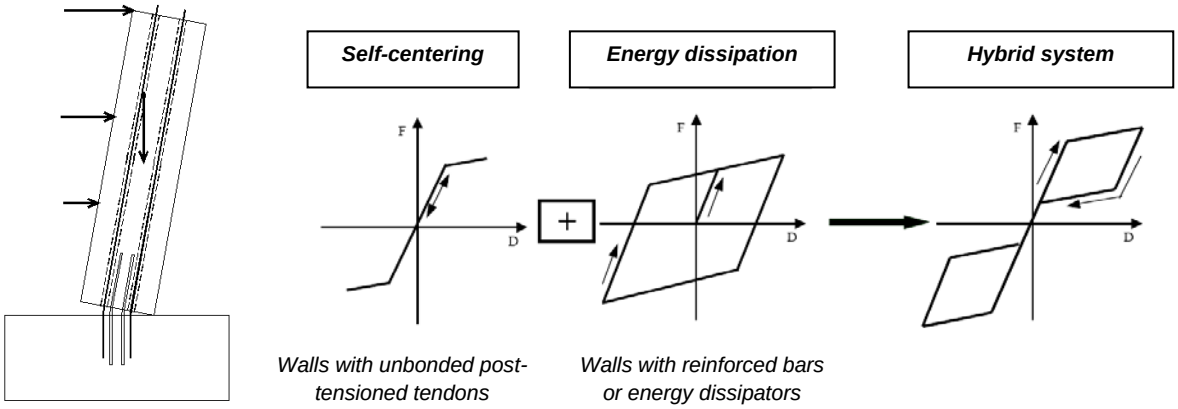

Fig. 1 – Self-centering wall and idealized hysteretic behavior of hybrid system [6].

2. Experimental Program

2.1 Structural systems

Three test units—miniature buildings with steel frames and concrete walls—were tested. The building was conceived as "miniature" (not "reduced scale") to resemble behavioral characteristics typical of a five-story dual system building. Because of this reason, no scaling factors were employed. Two of these test units, termed A1 and A2, had self-centering structural walls. One test unit, termed E1, had a structural wall fixed to the base and was designed as a conventional wall–frame system. The frames and walls were connected by rigid steel elements at each level to transfer inertia forces. Steel ingots over the metal bases were used to represent the mass of the building at each level. The ingots were connected in their upper sides by a steel plate to form a rigid diaphragm [9]. Fig. 2a shows a view of test unit A2 in the shaking table before testing. Longitudinal frames (parallel to the test direction) with replaceable steel pieces, called fuses, were used, located at the ends of beams and at the bases of the columns, in the zones of possible formation of plastic hinges (see Fig. 2b). This type of steel frame with fuses was first constructed at the University of Canterbury, New Zealand [10], and a frame with similar characteristics was constructed at the National University of Mexico (UNAM) and used in previous experimental research [11, 12]. The fuses were designed to have the stiffness, strength and energy dissipation capacity required to reach the required level of inelastic behavior. The conventional-wall test unit E1 was built with reinforced concrete, and its design was carried out using the Complimentary Technical Codes for Design of Concrete Structures of the Federal District (2004), which is based on ACI-318-2002. The self-centering walls of test units A1 and A2 were built with reinforced concrete, unbonded post-tensioning tendons and energy-dissipating reinforcement at the base of the wall. The design of these walls was based on recommendations by Restrepo and Rahman [6] and ACI-ITG-5.2-09 [13].

The walls were designed with a specified concrete compressive strength, f'_c, equal to 34.3 MPa and with a reinforcing steel having a specified yield stress f_y, equal to 412 MPa, for ASTM A615-type reinforcement and energy-dissipating reinforcement. The frame fuses were designed with A36-type steel. The prestressing tendons of test units A1 and A2 were wires designed with a specified tensile strength, f_{pu}, equal to 1,670 MPa.

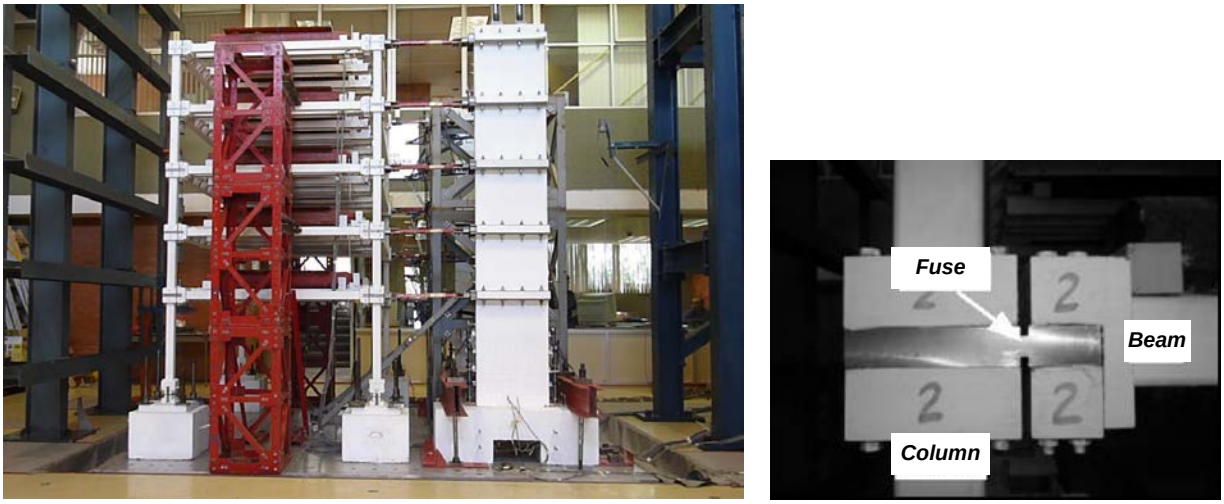

(a) View of test unit A2. (b) Detail of fuse.

Fig. 2 – View of test unit in the shaking table before testing and detail of fuse in beam-column joint.

The test units were designed using the elastic design spectrum of the Guerrero State Seismic Code for dense soil, the Acapulco Zone and ordinary buildings (Fig. 3). The spectral ordinate used was that of the plateau zone. The seismic behavior reduction factor was equal to 2, and the maximum allowable drift was 0.012. The seismic coefficient for design was therefore equal to 0.25. It must be pointed out that the elastic design spectrum specified in the Guerrero State is implicitly divided by the overstrength factor, Ω_D, therefore this spectrum must be multiplied by Ω_D to get the true elastic design spectra. For the sake of simplicity, in this study Ω_D was taken equal to 2.

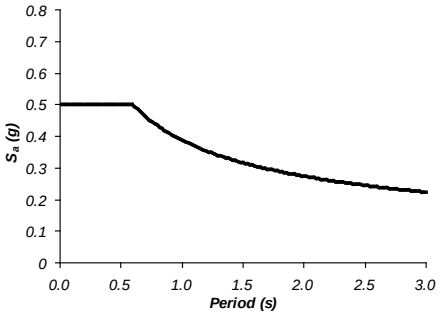

Fig. 3 – Design spectrum.

2.2 Materials and geometry

Test unit A1 was built with two steel frames and one self-centering concrete wall. The wall was designed to have a participation of 30% of the design base overturning moment. The actual mechanical properties of the materials are shown in Table 1. The wall had a transverse section of 0.35x0.09 m, and two 6-mm-diameter prestressing wires. The post-tensioning stress in test unit A1 at time of testing was equal to 0.45 f_{pu}. The wall had two 6-mm-diameter energy-dissipating bars, which were prepared using 9.5-mm-diameter deformed bars milled in segments 65 mm long to generate dog-bone-type dissipators with plain surfaces (see Fig. 4). The total weight of

the test unit was equal to 67.9 kN. Fig. 4 shows elevation and plan drawings of the test unit, as well as wall's transverse sections and reinforcement details.

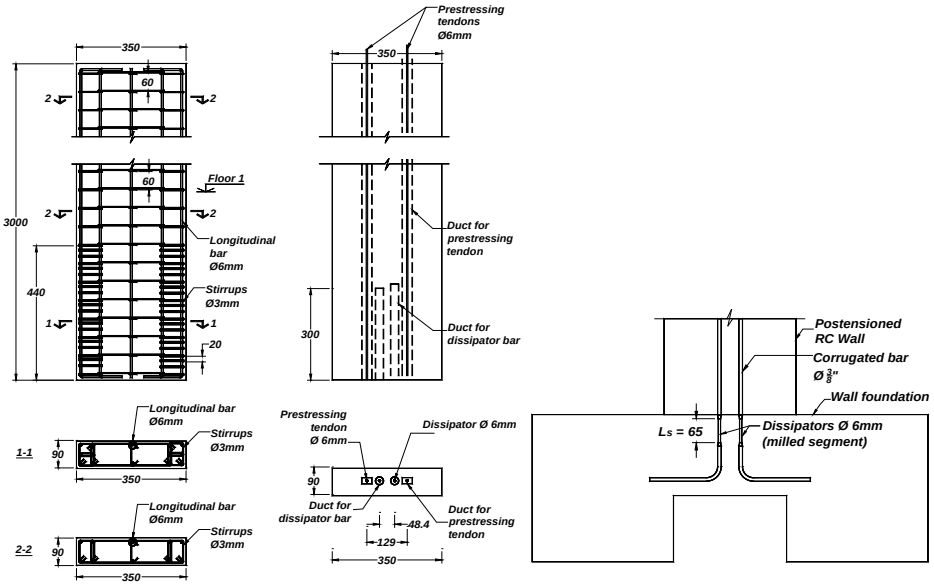

Fig. 4 – Test unit A1, dimensions in mm. Wall's transverse sections and reinforcement details.

Test unit A2 was built with two steel frames and two self-centering concrete walls. The walls were designed to have a total participation of 60% of design base overturning moment. Each wall had a transversal section of 0.55x0.09 m, two 7 mm-diameter prestressing wires and 7 mm-diameter dissipater bars. The actual mechanical properties of materials are shown in Table 1. Energy-dissipating reinforcement was prepared with 12.7 mm-diameter deformed bars milled in a segment of 100 mm-long to generate the dog-bone type dissipators, see Fig. 5. The post-tensioning stress in test unit A2 at time of testing was equal to 0.30 f_{pu}. Total weight of the test unit was equal to 73.7 kN. Fig. 5 shows elevation and plan of test unit, as well as walls' transversal sections and reinforcement details.

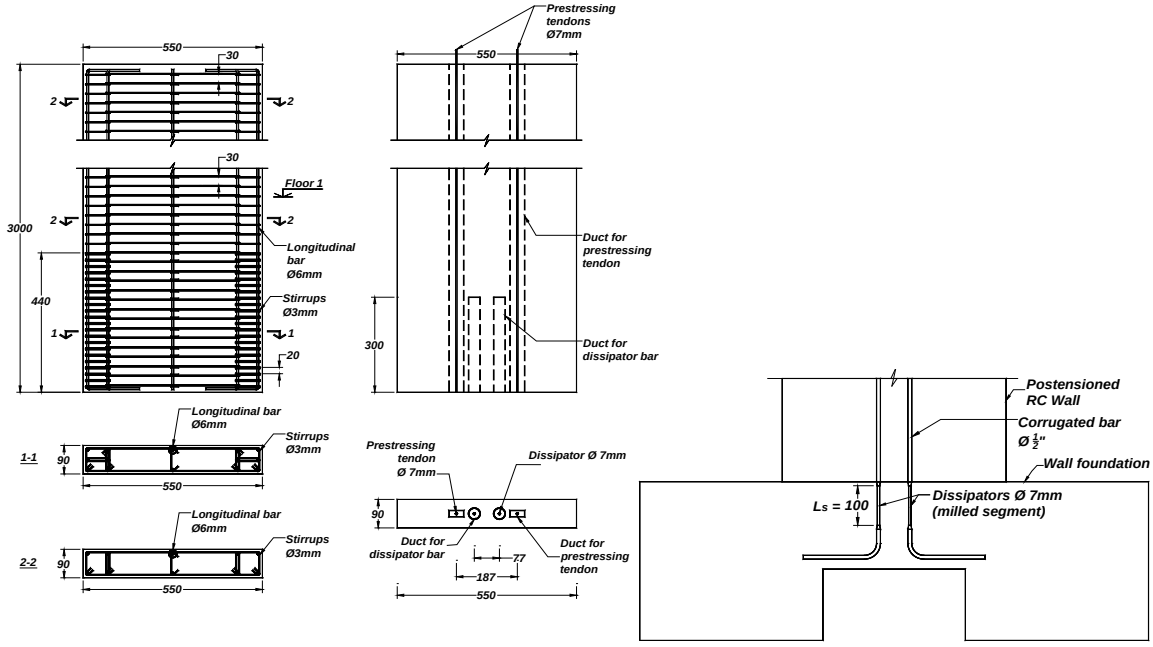

Fig. 5 – Test unit A2, dimensions in mm. Wall's transverse sections and reinforcement details.

Test unit E1 was built with two steel frames and one conventional concrete wall designed to have a participation of 50% of the design base overturning moment. The actual mechanical properties of the materials are shown in Table 1. The wall had a transverse section of 0.25x0.08 m. The total weight of the test unit was equal to 67.9 kN. Fig. 6 shows plan drawings of test unit E1, as well as the wall's transverse sections and reinforcement details.

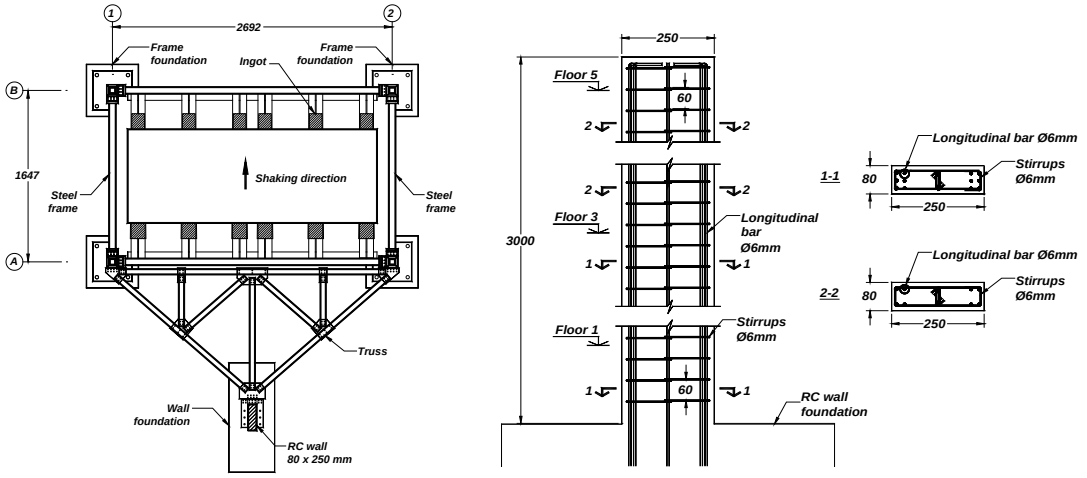

Fig. 6 – Test unit E1, dimensions in mm. Plan and wall's transverse sections and reinforcement details.

Table 1 – Actual mechanical properties of materials used in test units (measured at test time).

Material property	E1	A1	A2
Compressive strength of concrete (MPa)	47.1	44.1	48.1
Yield stress of reinforcement bars (MPa)	480.2	480.2	480.2
Yield stress of dissipator bars (MPa)	-	431.6	431.6
Yield stress of frame fuses (MPa)	307.7	313.9	269.8
Tensile stress of prestressing steel (MPa)	-	1802.1	1758.0

2.3 Test program

The tests carried out for every test unit were the following: ambient vibration, free vibration, low-intensity motion (elastic behavior), high-intensity motion and very-high-intensity motion. A relevant result in ambient vibration and free vibration tests is the measured fundamental period of each test unit. Other important results are the period of the second mode of vibration and the damping ratio of the structural system. These results were used in the calibration of analytical models of elastic behavior.

The earthquake input ground motion used in the shaking table tests was the accelerogram recorded at Llolleo Station, component EO, during the 1985 Chile earthquake. The earthquake input ground motion was not scaled, because the test units were of the miniature type, and therefore, no laws of similitude were employed. Fig. 7a depicts the Llolleo record, and Fig. 7b depicts the pseudoacceleration response spectrum of the Llolleo record for a 5% damping ratio (termed Llolleo-5%), as well as the specified elastic design spectrum (termed NTCS), and the true elastic design spectrum obtained with the ordinates of the later spectrum multiplied by the factor Ω_D =2 (termed NTCSx2). The use of the Llolleo record was considered appropriate since, for the fundamental periods of the test units before the high-intensity motions (about 0.3 s to 0.4 s) and slightly beyond, the differences between the ordinates of the elastic design spectrum and those of the Llolleo record are not significant (Fig. 7b).

The test units E1, A1 and A2 were subjected to the Llolleo record, termed High-intensity motion, and followed in test units A1 and A2 with an additional test run of increased intensity, termed Very-high-intensity motion.

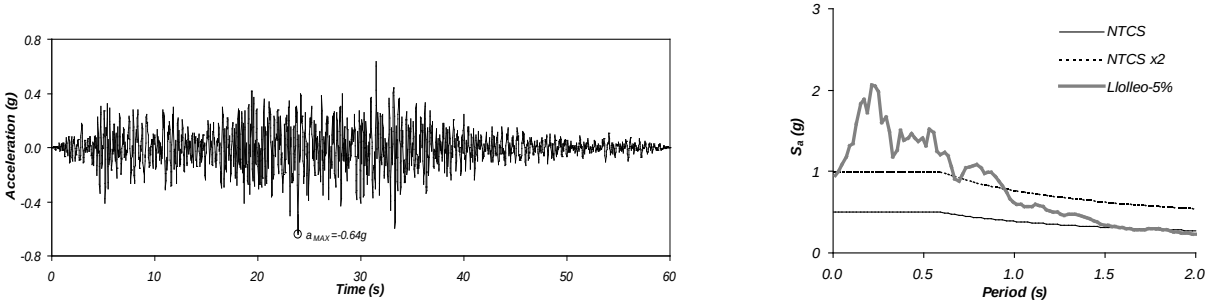

(a) Earthquake input ground motion, Llolleo 1985. (b) Response spectrum and design spectra.

Fig. 7 – Ground motion and response spectrum for Llolleo 1985, and design spectra.

The recorded peak ground accelerations (PGA) for the high-intensity motions were 0.93 g, 0.61 g and 0.71 g for test units E1, A1 and A2, respectively. However, an acceptable agreement was found between measured and objective earthquake input ground motions by comparison of elastic spectra from these motions [14]. After unit A1 was tested using the high-intensity motion, it was subjected to a test run of increased intensity, in which the accelerations of the high-intensity motion were multiplied by a factor of 1.5, which is termed very-high-intensity motion. For unit A2, a similar procedure was followed but using a factor of 1.25. The recorded PGA for the very-high-intensity motions were 1.0 g, and 0.89 g for test units A1 and A2, respectively.

3. Evaluation of results

Fig. 8 shows the measured floor acceleration envelopes, divided by PGA, versus the relative building height. Test units A1 and E1 have similar envelopes (Fig. 8a), except for the amplification at the roof level, which is greater for test unit E1. This difference was due to an unintentional slackness in the truss that connected the frame and the wall at the roof level. For high-intensity earthquakes, the maximum roof drift ratios were equal to 3.6%, 2.8% and 2.9% for test units E1, A1 and A2, respectively. For very-high-intensity earthquakes, the maximum roof drift ratios were equal to 4.1% in test units A1 and A2. Fig. 9 shows plots with measured interstory drift ratio envelopes versus the relative building height. This figure shows that the maximum measured interstory drift ratios in test units A1 and A2 are approximately constant along the building height at each test, a feature that can be found in typical dual systems. The interstory drift ratio envelope measured in test unit E1 shows a departure from the described envelope for test units A1 and A2.

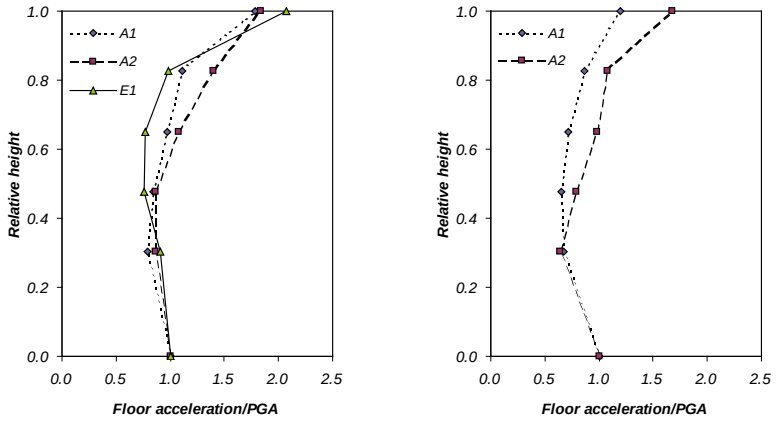

(a) High-intensity earthquakes. (b) Very-high-intensity earthquakes.

Fig. 8 – Floor acceleration envelopes.

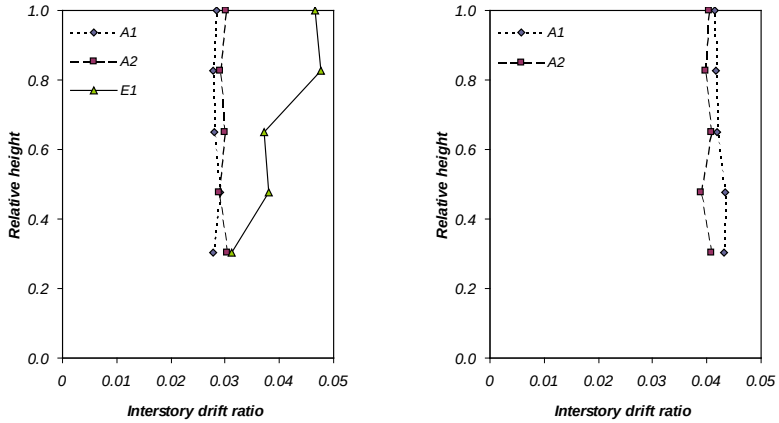

(a) High-intensity earthquakes. (b) Very-high-intensity earthquakes.

Fig. 9 – Measured interstory drift ratio envelopes.

The seismic behavior of the test units in the inelastic range was evaluated by estimating the R_M factor and the base shear overstrength factor, Ω_o. The R_M factor is a parameter that takes into account the global ductility and the effect of overstrength in the structure. The R_M factor represents a reduction in the seismic response, less influenced by higher-mode effects [14], and defined by the following expression:

$$R_M = \frac{M_{ve}}{M_{vo}} \tag{1}$$

M_{ve} is the maximum overturning moment demand in the building for elastic response to the earthquake input ground motion and M_{vo} is the maximum measured overturning moment of the building when responding in the inelastic range to that ground motion.

The base shear overstrength factor, Ω_o, is defined as the ratio of the maximum base shear to the design base shear. It is calculated from an approximation of the maximum base shear associated with the fundamental mode of vibration, V_o, according to the following expression:

$$V_o = \Omega_o \, C_S \, W \tag{2}$$

C_S is the seismic coefficient used in the building design.

Based on the assumption that the overturning moment is not influenced by higher-mode effects and that the effective height for the first mode, H_{eff}, does not change significantly during the inelastic response, the expression for the base shear overstrength factor is [14, 15]:

$$\Omega_o = \frac{M_{vo}}{H_{eff} \, C_S \, W} \tag{3}$$

With the acceleration records measured from high-intensity motions, the values of the R_M factor for test units E1, A1 and A2 were equal to 2.2, 3.0 and 2.5, respectively. These values show that the test units exhibited significant inelastic behavior. For the very-high-intensity motions, the experimental values of R_M were 4.4 and 3.0 for test units A1 and A2, respectively, which indicates major inelastic behavior. For high-intensity motions, the values of R_M obtained from experimental measurements of test units E1 and A1 are different because of the unexpected high acceleration recorded on the roof level of test unit E1. Based on a nonlinear dynamic analysis of test unit E1 using a calibrated analytical model, a value of R_M equal to 3.2 was calculated [15].

The values of the factor Ω_o were calculated using experimental results in the case of test units A1 and A2, and using analytical results in the case of test unit E1. For high-intensity motions, Ω_o for test units E1, A1 and A2

was equal to 2.0, 2.1 and 2.9, respectively. For very-high-intensity motions, Ω_o in A1 and A2 were equal to 2.3 and 3.0, respectively.

Test units A1 and E1 had similar values for the Ω_o and R_M factors. These test units were characterized by similar wall participation in the total base overturning moment. This suggests that for low-rise buildings it may be feasible to assess seismic design criteria for wall–frame dual systems with self-centering walls in a manner similar to that for conventional wall–frame systems. The test unit A2 reached greater base shear overstrength, associated with major wall participation in the total base overturning moment.

Fig. 10 depicts floor spectra for the roof level of test units for the low-intensity and high-intensity motions. The floor spectrum was defined as a pseudoacceleration response spectrum (S_a) calculated from the response of elastic oscillators with a 2% critical damping ratio, subjected to a base movement equal to the measured acceleration at the roof level of each test unit, divided by PGA. In each figure, two spectra are shown, the thin line representing the floor spectrum calculated from the measured roof accelerations of the test unit in elastic response and the thick line representing the floor spectrum calculated from the measured roof accelerations of the test unit in inelastic response. In addition, the periods of two first modes of vibration for the elastic response are shown as vertical lines. As seen in Fig. 10, the inelastic behavior of the test units leads to a higher reduction of response around the first mode of response. These results also show that the second mode of response is less affected by inelastic response at lesser degree than that for the first mode of response. Similar results have been found in other works [16, 17].

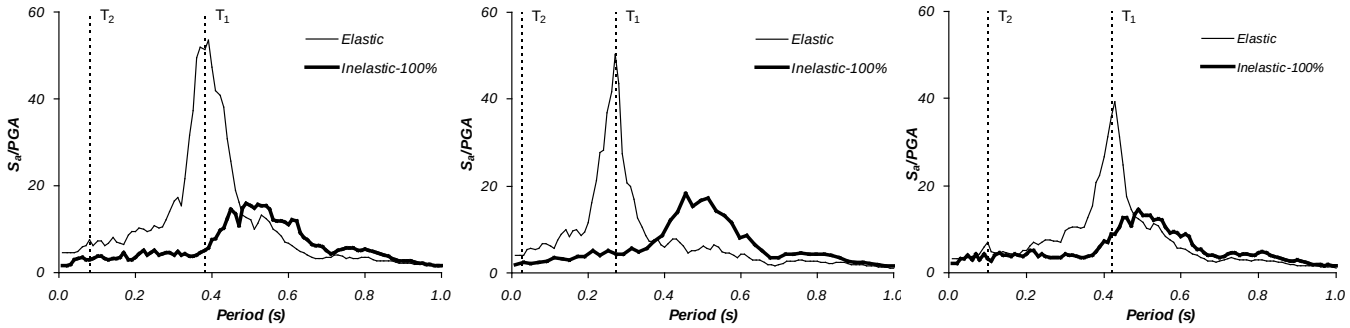

(a) A1. (b) A2. (c) E1

Fig. 10 – Floor spectra for measured accelerations at the roof level for low-intensity (elastic behavior) and high-intensity (inelastic behavior) motions.

Fig. 11a shows the relationships between residual interstory drift and maximum interstory drift for each test unit, for all the earthquake input ground motions in the experimental program. After the high-intensity motions, the maximum residual interstory drifts in test units A1 and A2 were equal to 0.19% and 0.17%, respectively, while for test unit E1, the maximum residual interstory drift was equal to 0.88%. As expected, the higher the maximum interstory drift was, the higher residual interstory drift was. However, as the seismic intensity increases, the residual interstory drift of a test unit with greater self-centering wall participation (test unit A2) is less than the residual interstory drift of a test unit with less self-centering wall participation (test unit A1). After the very-high-intensity motions, the residual interstory drift in test unit A2 was equal to 0.30%, while for test unit A1, the residual interstory drift was equal to 0.54%, or 1.8 times the value obtained for test unit A2, see Fig. 11a. This global trend in residual drifts was also observed in the permanent local rotations of critical sections of every test unit frame. Fig. 11b shows the residual and maximum rotations in the bases of columns and the ends of second-floor beams for every event experienced by the test units.

As seen in Fig. 11b, when comparing a dual system using a self-centering wall and other dual system using a conventional wall, the former leads to a significant decrease in residual deformations in critical sections of frame elements of the system. These results show that an increase in self-centering wall participation in total seismic response leads not only to a decrease in building residual drifts but also to a decrease in residual deformations in critical sections of frame elements.

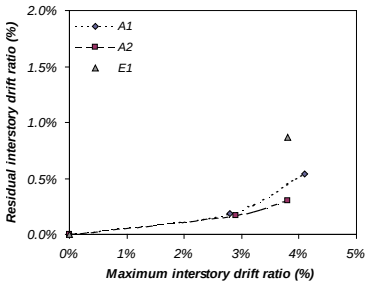

(a) Residual and maximum interstory drift ratio.

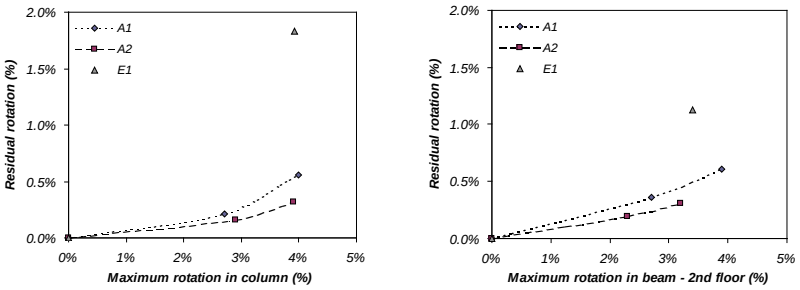

(b) Residual and maximum rotation in critical sections of frames.

Fig. 11 – Maximum drift and residual deformation in the test units.

For test units A1 and A2, damage was observed at the self-centering wall bases and at plastic hinges in the frame fuses, as expected. For the very-high-intensity motion test of test unit A1, the maximum rotation ductility demands were equal to 6.3 in beams and 7.1 in columns, and for test unit A2, the maximum rotation ductility demands were equal to 6.6 in beams and 7.1 in columns. Figs. 11a and 11b shows details of the final state of the wall bases in test units A1 and A2, respectively, at the end of the very-high-intensity motion tests. In both test units, spalling of the concrete cover and crushing of confined concrete over a length of approximately 50 mm was observed [15]. After test unit E1 was subjected to the high-intensity motion, plastic hinges at the wall base and at frame fuses were noted, with maximum rotation ductility demands equal to 4.9 in beams and 5.2 in columns. Cracks were observed along the wall height from the base up to 2.5 times the wall length, as shown in Fig. 12c. This figure also shows the rotation of the beam fuse after the high-intensity test of unit E1. At the wall base, 0.5-mm-wide cracks were observed [12].

(a) A1. (b) A2. (c) E1

Fig. 12 – View of the final state of the wall bases in test units.

4. Conclusions

The test units with self-centering walls exhibited seismic behavior comparable to that of the test unit with the conventional wall, in terms of maximum absolute accelerations, relative displacements, overstrength and ductility reduction factors. This behavior was more evident for the test units A1 (self-centering) and E1 (conventional), which were designed to have similar degrees of wall participation in the total seismic response in terms of the base overturning moment. In addition, in the test units with self-centering walls, a decrease in residual deformations in the critical sections of the frame elements was observed. The proportion of this decrease was similar to that observed in the building's residual drifts. In addition, the inelastic behavior of the test units with self-centering walls leads to a higher reduction of the response around the first mode of vibration, as observed in the test unit with conventional wall and other frame systems.

The experimental results show that dual systems with self-centering walls have in general a behavior in a manner similar to dual systems with conventional walls, with the additional benefit of reduced residual drifts. These results suggest the possibility in low-rise buildings of using seismic design criteria similar to those used for wall–frame dual systems with conventional walls for wall–frame dual systems with self-centering walls.

5. Acknowledgements

The financial support of the Program of Science and Technology (FINCYT) of the Government of Peru, the Latin American Scholarships Program for American Universities (LASPAU) and the National University of Engineering (UNI) of Peru are gratefully acknowledged. The support of UC MEXUS-CONACYT, Grant Number CN-09318, which made it possible to conduct some of the tests described in this paper, is also acknowledged. Thanks are due to Professor José I. Restrepo of the University of California at San Diego, for his critical review of this work.

6. References

[1] Priestley M.J.N. and Tao J.R. (1993), "Seismic response of precast prestressed concrete frames with partially debonded tendons", *PCI Journal*, pp. 58-69, January-February 1993.

[2] Priestley, M.J.N. (1996). "The PRESSS Program – Current status and proposed plans for phase III", *Special report, PCI Journal*, March-April 1996.

[3] Priestley M.J.N. Sritharan, S., Conley, J, and Pampanin, S. (1999), "Preliminary results and conclusions from the PRESSS five-story precast concrete test building", *PCI Journal, Special Report*, Vol. 44, No.6, pp. 42-67.

[4] Kurama, Y., Sause, R., Pessiki, S. and Lu, L.W. (1999). "Lateral load behavior and seismic design of unbonded post-tensioned precast concrete walls", *ACI Structural Journal*, Vol.96, No.4, pp. 622-633.

[5] Holden, T, Restrepo, J. and Mander, J. (2003). "Seismic performance of precast reinforced and prestressed concrete walls", *Journal of Structural Engineering ASCE*, Vol. 129, No.3, pp. 286-296.

[6] Restrepo, J. and Rahman, A. (2007). "Seismic performance of self-centering structural walls incorporating energy dissipators", *Journal of Structural Engineering ASCE*, Vol.133, No.11, pp. 1560-1570.

[7] Perez, F., Sause, R., and Pessiki S. (2007), "Analytical and experimental lateral load behavior of unbonded postensioned precast concrete walls", *Journal of Structural Engineering ASCE*, Vol.133, No.11, pp. 1531-1540.

[8] Aaleti, S, and Sritharan, S. (2009). "A simplified analysis method for characterizing unbounded post-tensioned precast wall systems", Engineering Structures, Vol. 31, pp. 2966-2975. Elsevier Ltd. doi: 10.1016/j.engstruct.2009.07.02.

[9] Rodríguez, M.E., Restrepo, J. and Blandón, J., (2006). "Shaking Table Tests of a Four-Story Miniature Steel Building-Model Validation". Earthquake Spectra, EERI, Vol 22, No 3, pp. 755-780.

[10] Kao, G. (1998). "Design and shake-table test of a four-storey miniature structure built with replaceable plastic hinges", Master Thesis, Department of Civil Engineering, University of Canterbury. Christchurch, New Zealand.

[11] Blandón, J. (2006). "Diseño sísmico de sistemas de piso en estructuras prefabricadas de concreto" (in Spanish), Ph.D. Thesis, Faculty of Engineering, National University of Mexico, Mexico.

[12] Sánchez, R. (2008). "Diseño sísmico de edificios con sistemas duales regulares" (in Spanish), Ph.D. Thesis, Faculty of Engineering, National University of Mexico, Mexico.

[13] ACI Innovation Task Group 5 (2009). "Requirements for design of special unbonded post-tensioned precast shear wall satisfying ACI ITG-5.1 (ACI ITG-5.2-09) and Commentary", American Concrete Institute, Farmington Hills, MI.

[14] Salinas, R., Rodríguez, M.E., and Sánchez, R. (2013). "Ensayes en mesa vibradora de edificios miniatura con muros estructurales de concreto convencionales y autocentrados" (in Spanish), *Revista de Ingeniería Sísmica SMIS*, No. 89, pp. 101-134.

[15] Salinas, R. (2013). "Evaluación del desempeño sísmico de sistemas estructurales innovadores" (in spanish), Ph.D. Thesis, Faculty of Engineering, National University of Mexico, Mexico.

[16] Rodríguez, M.E., Restrepo, J. and Carr, A., (2002). "Earthquake induced horizontal floor accelerations in buildings", *Earthquake Engineering and Structural Dynamics*, Vol. 31, pp. 693-718.

[17] Rodríguez, M.E., Restrepo, J. and Blandón, J., (2007). "Seismic design forces for rigid floor diaphragms in precast concrete buildings structures", *Journal of Structural Engineering ASCE*, Vol. 133, No. 11, pp. 1604-1615.